Calculation of electron scattering from the ground state of ytterbium

Christopher J. Bostock,* Dmitry V. Fursa, and Igor Bray
ARC Centre for Antimatter-Matter Studies, Curtin University, GPO Box U1987, Perth, WA 6845, Australia
(Received 29 March 2011; published 24 May 2011)

We report on the application of the convergent close-coupling method, in both relativistic and nonrelativistic formulations, to electron scattering from ytterbium. Angle-differential and integrated cross sections are presented for elastic scattering and excitation of the states $(6s6p)^3P_{0,1,2}$, $(6s6p)^1P_1^o$, $(6s7p)^1P_1^o$, and $(6s5d)^1D_2^e$ for a range of incident electron energies. We also present calculations of the total cross section, and angle-differential Stokes parameters for excitation of the $(6s6p)^3P_1^o$ state from the ground state. A comparison is made with the relativistic distorted-wave method and experiments.

DOI: 10.1103/PhysRevA.83.052710 PACS number(s): 34.80.Bm, 34.80.Dp, 34.80.Nz

I. INTRODUCTION

Electron scattering from ytterbium has attracted renewed attention. A series of experiments at the University of Manitoba has been conducted to study electron scattering from the laser-excited 6^3P_1 level of ytterbium where differential cross sections (DCS) [1] and P_3 Stokes parameter [2] have been measured for a number of transitions. A similar superelastic scattering technique has been used in earlier experiments by the same group to study P_1, P_2, and P_3 Stokes parameters for the 6^3P_1–6^1S_0 transition [3,4]. These experiments rely on the possibility of preparing the 6^3P_1 state of ytterbium by laser pumping from the ground state. This indicates a breakdown of the nonrelativistic approximation for this relatively heavy atom ($Z = 70$) and illustrates the need to apply advanced relativistic scattering theories to study electron scattering from ytterbium.

The University of Manitoba experiments have been augmented by the results of a number of theoretical approaches, such as the relativistic distorted-wave approximation (RDWA), relativistic convergent close-coupling (RCCC), and convergent close-coupling (CCC) methods. It was found [1,2] that the RCCC method offers a better agreement with experiments than the RDWA and CCC methods, although the agreement is far from perfect. It is therefore worthwhile to conduct a detailed study of electron scattering from ytterbium to investigate the accuracy of the RCCC method in comparison to other theoretical approaches using a much larger set of experimental results. Electron scattering from the ground state of ytterbium offers a good opportunity to achieve this.

Several experimental studies of electron scattering from ytterbium exist. Shimon *et al.* [5] measured optical excitation functions for a large number of transitions in Yb and Yb^+. The Belgrade group, Predojević *et al.* [6,7], measured differential cross sections for elastic scattering, and excitations of $(6s6p)^1P_1^o$, $(6s6p)^3P_1^o$, $(6s6p)^3P_2^o$, $(6s5d)^1D_2^e$, and $(6s7p)^1P_1^o$ states at a number of incident electron energies (10–80 eV) and a wide range of scattering angles. Estimates of integrated cross sections for these transitions have also been presented. Differential cross sections for excitation of the $(6s6p)^1P_1^o$ state and $(6s6p)^3P_{0,1,2}^o$ state have been measured by Johnson *et al.* [8] and Zetner *et al.* [4], respectively. We note a large disagreement between Predojević *et al.* [6] and Johnson *et al.* [8] in the normalization of differential cross sections to absolute values. The issue of normalization of DCS measurements will be addressed in Sec. III.

Previous theoretical studies of e-Yb scattering, aside from our close-coupling calculations, include first-order perturbative methods and optical potential methods. Srivastava *et al.* [9] presented RDWA calculations of Stokes parameters for the $J = 1$ states, and differential cross sections for the $(6s6p)^3P_1$ and $(6s6p)^1P_1^o$ states. Unitarized distorted-wave approximation (UDWA) calculations have been presented by Johnson *et al.* [8] for $(6s6p)^1P_1$ differential cross sections and Zetner *et al.* [4] for differential cross sections and electron-impact coherence parameters for the $(6s6p)^3P_J$ levels. Differential cross sections for elastic electron scattering on Yb calculated using an optical potential approximation have been reported by Kelemen *et al.* [10,11] and Neerja *et al.* [12].

The paper is organized as follows: Sec. II contains a brief overview of the RCCC and CCC methods, with details applicable to electron scattering from ytterbium. In Sec. III we present results of our calculations for angle-differential and integrated cross sections across a range of incident electron energies for elastic scattering and excitation of the states $(6s6p)^3P_{0,1,2}$, $(6s6p)^1P_1^o$, $(6s7p)^1P_1^o$, and $(6s5d)^1D_2^e$. We also present the results of total cross-section calculations and angle-differential Stokes-parameter calculations for excitation of the $(6s6p)^3P_1^o$ state from the ground state of ytterbium. The RCCC and CCC results are compared with available experiments and other theoretical methods. Atomic units are used throughout the paper.

II. CALCULATION METHODS

A. RCCC method

The recently developed RCCC method has been applied to the calculation of electron scattering from quasi-one-electron targets [13–17] and quasi-two-electron targets [18]. In the latter case, it was applied to electron scattering from mercury, where the Hg atom ($Z = 80$) was modeled as an atom with two valence electrons above a $[Xe]4f^{14}5d^{10}$ closed core. A similarly structured model of two valence electrons above a frozen core is adopted for Yb, however, in this case, the core is $[Xe]4f^{14}$. In this paper, we present only a brief overview of the RCCC method for quasi-two-electron targets and refer

*c.bostock@curtin.edu.au

the reader to Bostock *et al.* [18] for details. The RCCC method solves the relativistic Lippmann-Schwinger equation in partial-wave form,

$$T_{fi}^{\Pi J}(k_f\kappa_f,k_i\kappa_i) = V_{fi}^{\Pi J}(k_f\kappa_f,k_i\kappa_i) + \sum_n \sum_\kappa \int\!\!\!\!\!\!- dk \frac{V_{fn}^{\Pi J}(k_f\kappa_f,k\kappa) T_{ni}^{\Pi J}(k\kappa,k_i\kappa_i)}{E-\epsilon_n^N-\epsilon_{k'}+i0}, \quad (1)$$

where the notation is described in detail in [14], and starts from a multi-electron Dirac-Coulomb Hamiltonian in the no-virtual-pair approximation [13]. The [Xe]$4f^{14}$ Dirac-Fock core orbitals are obtained using the GRASP package [19]. For the valence electrons, a set of one-electron orbitals is obtained by diagonalization of the Yb^+ quasi-one-electron Dirac-Coulomb Hamiltonian in a relativistic (Sturmian) L-spinor basis [20]. The set of orbitals obtained resembles closely the corresponding nonrelativistic one-electron basis and contains $6s$–$12s$, $6p_j$–$12p_j$, $5d_j$–$10d_j$, and $5f_j$–$7f_j$ ($j = l \pm 1/2$) orbitals. Two-electron configuration-interaction calculations are then performed to obtain wave functions for the Yb atom. The choice of two-electron configurations was such that one electron is in $6s$,$6p_{1/2}$, or $6p_{3/2}$ orbitals, while the other electron occupies any of the one-electron orbitals allowed by selection rules. We have found that by limiting two-electron configurations to those that have one electron in the $6s$ or $6p$ orbitals, we can obtain a sufficiently accurate description of the Yb wave functions.

We have also added phenomenological one- and two-electron polarization potentials to improve the accuracy of the calculated Yb wave functions. The phenomenological one-electron $V^{\rm pol}$ and two-electron $V^{\rm diel}$ core polarization potentials allow us to take into account more accurately the effect of closed inert shells on the active electron [21]. The fall-off radius $r_c^{\rm pol}$ and $r_c^{\rm diel}$ of these potentials is chosen to obtain the best representation of target state energies and optical oscillator strength (OOS), while the static dipole polarizability of the inert core α_c is taken either from experiment or accurate calculations. In the case of Yb, we chose $\alpha_c = 28.4$, $r_c^{\rm diel} = 4.06$, and an l-dependent $r_c^{\rm pol}$ with values 3.7, 3.9, 3.4, and 3.7, for $l = 0,1,2$, and 3, respectively. The energy levels of the first 10 states used in the calculation are listed in Table I, and the OOSs for the $(6s6p)^3P_1$ and $(6s6p)^1P_1$ states are listed in Table II.

The fully relativistic approach leads to a large number of states, with 301 states in the present calculations, and consequently to significantly larger close-coupling calculations compared to the nonrelativistic approach (discussed in the next section). However, it allows us to obtain accurate results for transitions between fine-structure levels of target atoms and ions, which is of particular importance for the present work. For some integrated cross sections, we compare the RCCC calculations for the 301 states (labeled RCCC 301) with 49 state calculations (labeled RCC 49) that include only the bound states. This comparison will illustrate the effect of coupling on the continuum.

TABLE I. Energy levels of the first 10 Yb states calculated by diagonalizing the target in the RCCC and CCC methods. Experiment levels listed by NIST [24] are also shown.

			Energy (eV)			
Configuration	Term	J	Parity	RCCC	CCC	Experiment
$6s^2$	$^1S_0$	0.0	1	0.000	0.000	0.000
$6s6p$	$^3P_0^o$	0.0	−1	2.09	2.24	2.143
$6s6p$	$^3P_1^o$	1.0	−1	2.16	2.30	2.231
$6s6p$	$^3P_2^o$	2.0	−1	2.37	2.44	2.444
$6s6p$	$^1P_1^o$	1.0	−1	3.02	3.03	3.108
$5d6s$	$^3D_1$	1.0	1	2.96	2.83	3.036
$5d6s$	$^3D_2$	2.0	1	2.97	2.87	3.069
$5d6s$	$^3D_3$	3.0	1	2.97	2.94	3.133
$5d6s$	$^1D_2$	2.0	1	3.56	3.60	3.432
$6s7s$	$^3S_1$	1.0	1	4.07	4.08	4.054
Ionization limit				6.25	6.22	6.254

B. CCC method

The CCC method and its application to electron scattering from quasi-two-electron atoms has been described in [22]. Similar to the RCCC method, we model the Yb atom as a system with two active electrons above a closed Hartree-Fock core. The core orbitals are obtained via the self-consistent Hartree-Fock computer program of Chernysheva *et al.* [23]. By diagonalizing the Hamiltonian of the Yb^+ ion in a large Sturmian (Laguerre) basis, we obtain a set of one-electron orbitals: $6s$–$12s$, $6p$–$12p$, $5d$–$10d$, and $5f$–$7f$. These orbitals have then been used in a standard two-electron configuration-interaction calculation in order to obtain a set of Yb atom wave functions. The number of one-electron orbitals have been kept the same in both the RCCC and CCC calculations for ease of comparison between the models. One- and two-electron polarization potentials have been used to model more accurately core-valence electron correlations. The static dipole polarizability of the inert core α_c was chosen to be the same as in the RCCC model, while the fall-off radius of these polarization potentials has been chosen to obtain the ground-state energy and OOS for the resonance $(6s6p)^1P_1^o$–$(6s^2)^1S_0$ transition close to experimental values. Specifically we chose $r_c^{\rm diel} = 4.2$ and an l-dependent $r_c^{\rm pol}$ with values 3.0, 3.65, 3.65, and 3.65 for $l = 0,1,2$, and 3, respectively. A total of 150 states obtained in the Yb structure calculations are then used to perform a multichannel expansion of the total wave function for the e-Yb scattering system and solve the resulting set of momentum-space, partial-wave, close-coupling equations for the T matrix. The scattering amplitudes are calculated from the partial-wave T matrix in the usual way.

TABLE II. Optical oscillator strength of the Yb ground state. Experiment: (a) Ref. [25], (b) Ref. [26], (c) Ref. [27], and (d) Ref. [28].

	Optical oscillator strength			
Transition	RCCC	CCC	Experiment	
$(6s^2)^1S_0$–$(6s6p)^3P_1$	0.0125	0.0118	0.0183[(a)]	0.0163[(b)]
$(6s^2)^1S_0$–$(6s6p)^1P_1$	1.29	1.28	1.27[(c)]	1.30[(d)]

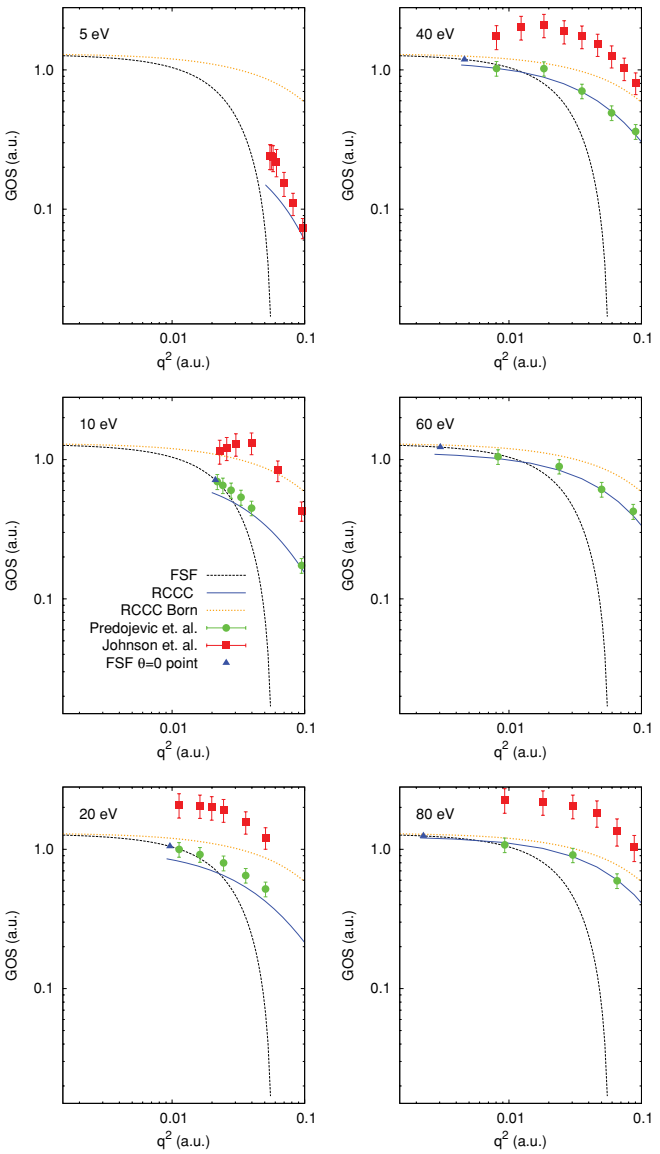

FIG. 1. (Color online) RCCC and CCC generalized oscillator strengths, and measurements from Predojević *et al.* [6] and Johnson *et al.* [8]. Also shown is forward-scattering function (FSF) $\phi(q^2)$ from Felfli and Msezane [32].

In order to take into account the major relativistic effect, which is singlet-triplet mixing in the Yb wave functions, we transformed calculated nonrelativistic scattering amplitudes to the intermediate coupling representation. Such an approach proved to be successful in the case of the heavier Hg atom [21] and is expected to perform equally well for Yb. Mixing coefficients have been obtained by diagonalizing the Breit-Pauli Hamiltonian with a one-electron spin-orbit term. The strength of the spin-orbit term has been adjusted to reproduce fine-structure splitting of the lowest lying states of the Yb^+ ion.

The energy levels of the first 10 states used in the calculations are listed in Table I, and the OOSs for the $(6s6p)^3P_1$ and $(6s6p)^1P_1$ states are listed in Table II.

Good agreement between theoretical results and experiment is found for both energy levels and OOS. We would like to

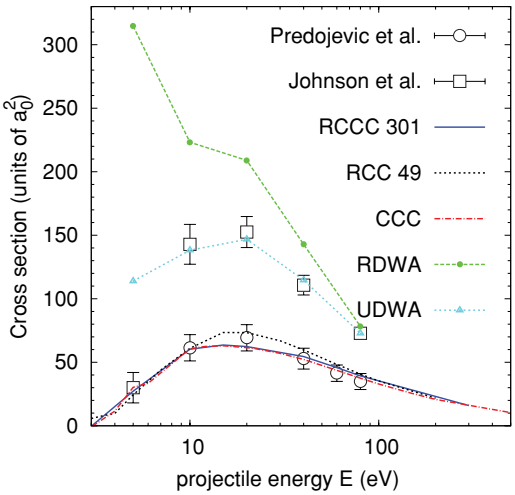

FIG. 2. (Color online) ICS for excitation of the $(6s6p)^1P_1^o$ state from the ground state of ytterbium. The measurements are from Predojević *et al.* [7] and Shimon *et al.* [5]. The UDWA calculations are from Johnson *et al.* [8], and the RDWA calculations are from Srivastava *et al.* [9].

emphasize that the OOSs are strongly affected by the two-electron polarization potential. If the two-electron polarization potential is not taken into account, then the OOS values for the resonance $(6s6p)^1P_1^o$–$(6s^2)^1S_0$ transition are much higher, with values $f = 2.0$ (RCCC) and $f = 2.2$ (CCC). We will see later that correct values of OOS are important for an accurate description of the differential and integrated cross sections for optically allowed transitions.

Another important parameter that allows us to evaluate the accuracy of the employed structure model of ytterbium is the static dipole polarizability of ytterbium. In our RCCC and CCC calculations, it is obtained via the following expression:

$$\alpha_d = \sum_n f_n/(2E_n)^2. \tag{2}$$

We obtain a value of $\alpha_d = 106$ in RCCC and $\alpha_d = 105$ in CCC calculations. It is dominated by the resonance transition and strongly dependent on its OOS value. The recommended value, $\alpha_d = 143$ [29], is substantially larger than the calculations of the RCCC or CCC methods. The error in static dipole polarizability could lead to underestimation of the forward-elastic-scattering cross sections. It is an indication of the deficiency of the target structure model (two active electrons above a frozen core) that we use to describe ytterbium. Excitations of the $4f^{14}$ core electrons are apparently important [30], however, they are not modeled explicitly in our calculations. The situation here is similar to our approach to the calculation of electron scattering from mercury [21,31]. In that case, excitations of the $5d^{10}$ core electrons were not allowed but were modeled via a two-electron polarization potential. Good agreement with the *e*-Hg experiment for DCS and integrated cross sections (ICS) for various transitions was obtained with the RCCC method, which gives us confidence in the application of a similar technique to ytterbium.

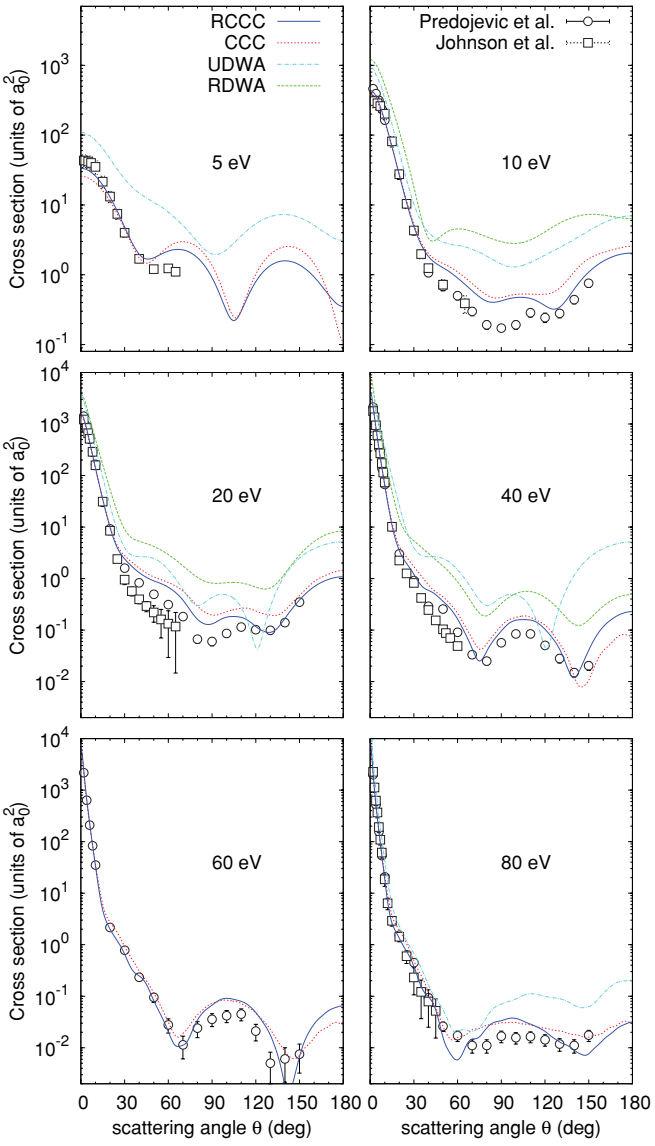

FIG. 3. (Color online) DCS for excitation of the $(6s6p)^1P_1^o$ state from the ground state of ytterbium at 10, 20, 40, 60, 80, and 100 eV incident electron energies. The measurements are from Predojević *et al.* [6] and Johnson *et al.* [8]. The RCCC and CCC calculations are described in the text, the UDWA calculations are presented in Johnson *et al.* [8], and the RDWA calculations are from Srivastava *et al.* [9].

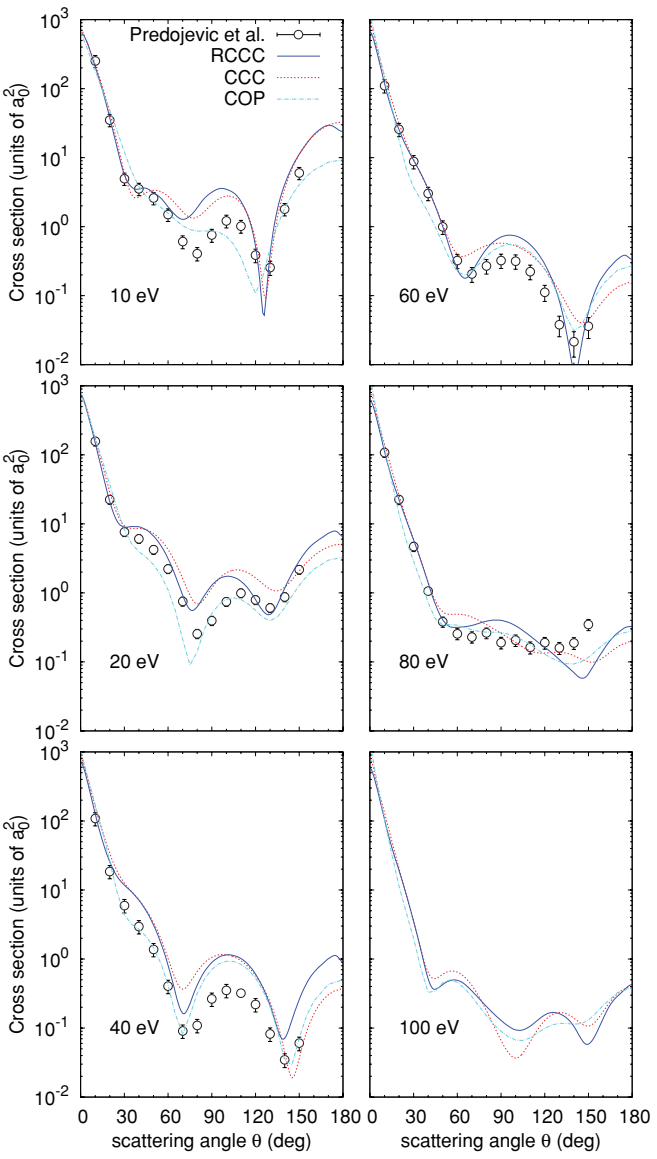

FIG. 4. (Color online) DCS for elastic scattering on the ground state of ytterbium at 10, 20, 40, 60, 80, and 100 eV incident electron energies. The measurements are from Predojević *et al.* [6]. The RCCC and CCC calculations are described in the text. The complex optical potential (COP) calculations are from Kelemen *et al.* [11].

III. RESULTS

We begin our comparison of the RCCC and CCC results with experiments by addressing the normalization of the DCS measurements of Predojević *et al.* [6] and Johnson *et al.* [8].

Predojević *et al.* [6] employed a normalization technique, based on the work of Felfli and Msezane [32], and Avdonina *et al.* [33], which involved the following steps. First, the experimental generalized oscillator strength (GOS) values are plotted against the squared momentum transfer (q^2) for each incident energy. Second, the forward-scattering function $\phi(q^2)$, which describes the locus of $\theta = 0^\circ$ GOS points at various incident electron energies, is plotted, and the $\theta = 0^\circ$ point is marked for the relevant incident energy. Finally, the experimental data is extrapolated to where it intersects the $\phi(q^2)$ curve. The experimental data is then normalized such that this point of intersection corresponds to the $\theta = 0^\circ$ point for that incident energy. The GOS values are related to the DCS values via the relation

$$f^{\mathrm{GOS}}(q,E) = \frac{w}{2}\frac{k_i}{k_f}q^2\left(\frac{d\sigma}{d\Omega}\right), \tag{3}$$

where q, E, w, k_i, and k_f are the momentum transfer, incident energy, excitation energy, and incident and scattered electron momenta, respectively. Note that this method is only valid for incident energies $E > 2.5\omega$ [32].

In Fig. 1, the RCCC generalized oscillator strength for the $(6s6p)^1P_1^o$ state is plotted as a function of the squared momentum transfer (q^2), and the corresponding experimental

values of Predojević *et al.* [6] are shown. At 10 eV, the analytical behavior and normalization of the experimental results are in relatively poor agreement with the RCCC results, particularly at forward-scattering angles. At 20 eV, the analytical behavior of the experimental GOS values is in much better agreement with the RCCC results, however, the absolute value of the normalization is not in agreement with the RCCC results. At 40 eV, there is relatively good agreement both in the analytical behavior and normalization between RCCC theory and experiment, and at 60 and 80 eV, we see very good agreement between the experimental and RCCC results.

We also note that the curve labeled "Born" in Fig. 1 indicates the high-energy limit, and as $q \to 0$ converges to the optical oscillator strength limit, $f = 1.29$ a.u. The close-coupling results are substantially below the Born limit at incident electron energies below 80 eV, which indicates that interchannel coupling is important and first-order methods might be inaccurate at low and intermediate energies.

We now compare the RCCC generalized strengths for the $(6s6p)^1P_1^o$ state with the experimental data of Johnson *et al.* [8], plotted in Fig. 1. At 5, 10, and 40 eV, the analytical behavior and normalization of the experimental values are in poor agreement with the RCCC results. At 20 and 80 eV, there is relatively good agreement in the analytical behavior of the experimental and RCCC results, however, the absolute value of the normalization is not in agreement with the RCCC results. Johnson *et al.* [8] normalized their data by utilizing the UDWA integrated cross sections at 80 eV, and then employing the optical excitation function data of Shimon *et al.* [5] to normalize their results at other energies. The critical issue with this approach is that the UDWA as well as the RDWA [9] substantially overestimate the $(6s6p)^1P_1^o$ DCS for two reasons. First, and most importantly, both UDWA and RDWA model Yb as an atom with two active electrons above a frozen core (the same model as in RCCC and CCC). However, no further modeling of core excitations (by means of two-electron polarization potential) has been done. As we discussed earlier, this leads to a large error (nearly a factor of two) in the OOS value for this $(6s6p)^1P_1^o$–$(6s^2)^1S_0$ resonance transition and, as a result, to a comparable error in the $(6s6p)^1P_1^o$ DCS. Second, both UDWA and RDWA are high-energy methods and their application at low and intermediate incident electron energies can lead to overestimation of the cross sections.

Predojević *et al.* [6] and Johnson *et al.* [8] used their DCS values to obtain integrated cross sections, as shown in Fig. 2. The RCCC and CCC results are in excellent agreement with each other, and they are also in good agreement with the experimental measurements of Predojević *et al.* [6]. The UDWA calculations of Johnson *et al.* [8], and the RDWA calculations of Srivastava *et al.* [9] are both significantly larger than the experiment as well as the RCCC and CCC calculations. The effect of coupling to the continuum is

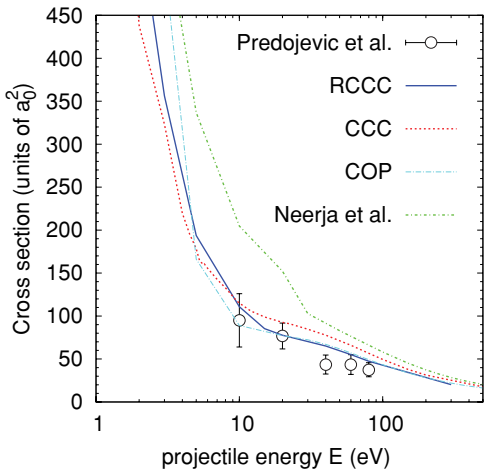

FIG. 5. (Color online) ICS for elastic scattering on the ground state of ytterbium. The measurements are due to Predojević *et al.* [7]. The RCCC and CCC calculations are described in the text. Also shown are calculations from Neerja *et al.* [12], and the complex optical potential (COP) calculations from [11].

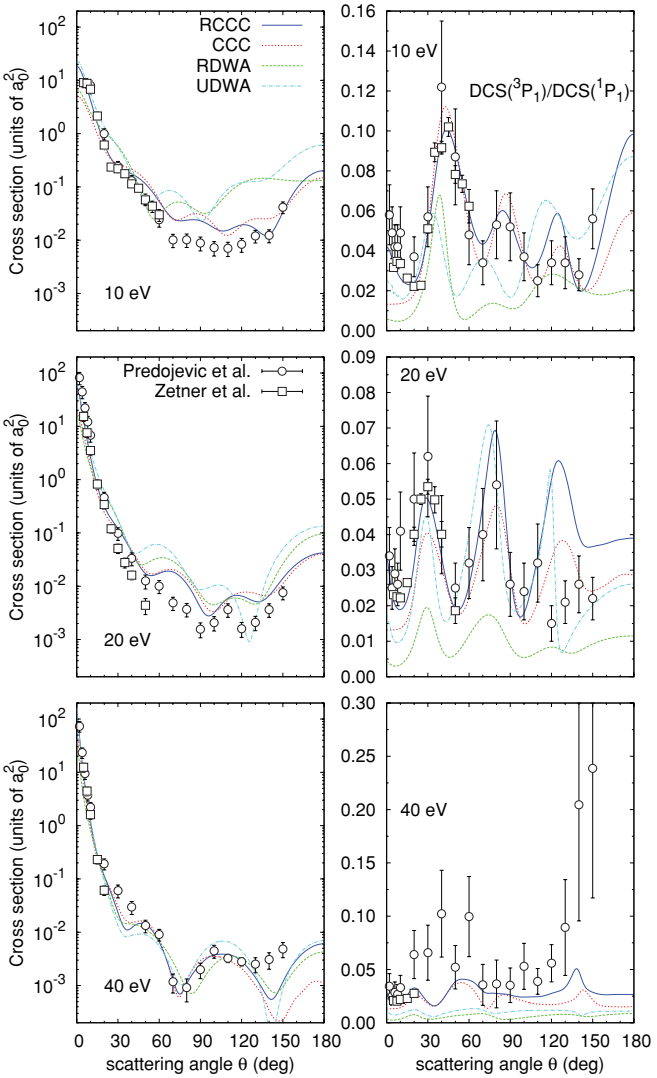

FIG. 6. (Color online) DCS for excitation of the $(6s6p)^3P_1^o$ state from the ground state of ytterbium and its ratio to the $(6s6p)^1P_1^o$ state DCS at 10, 20, and 40 eV incident electron energies. The measurements are from Predojević *et al.* [7] and Zetner *et al.* [4]. The RCCC and CCC calculations are described in the text, the UDWA calculations are presented in Zetner *et al.* [4], and the RDWA calculations are from Srivastava *et al.* [9].

TABLE III. Renormalization factors for the experimental measurements of Johnson *et al.* [8] based on $(6s6p)^1P_1^o$ integrated cross section (a_0^2).

Energy(eV)	RCCC	Johnson *et al.* [8]	Scaling factor
5	27.3	30.0	0.91
10	60.3	142.9	0.42
20	62.3	152.5	0.41
40	54.5	110.7	0.49
80	39.3	72.9	0.54

indicated; the RCC 49 calculations include only the bound states, which produce larger ICS.

In view of the discrepancies between the RCCC GOS and the results of Johnson *et al.* [8], in Table III we present the renormalization scale factors for the available experimental measurements in Johnson *et al.* [8] to aid in the comparison with the RCCC results. In all subsequent figures in this section, the results of Johnson *et al.* [8] and Zetner *et al.* [4] have been renormalized with these scaling factors.

The differential cross sections for excitation of the $(6s6p)^1P_1^o$ state from the ground state of ytterbium at 5, 10, 20, 40, 60, and 80 eV incident electron energies are presented in Fig. 3. There is generally excellent agreement between the RCCC and CCC results, which indicates that relativistic effects are of little importance for this transition. The experimental measurements of Johnson *et al.* [8] and Predojević *et al.* [6] are in relatively good agreement with the RCCC and CCC results.

In Fig. 4 we present the RCCC and CCC DCS results for elastic scattering on the ground state of ytterbium at 10, 20, 40, 60, 80, and 100 eV incident electron energies. There is generally good agreement between the RCCC and CCC calculations across all energies. We find very good agreement

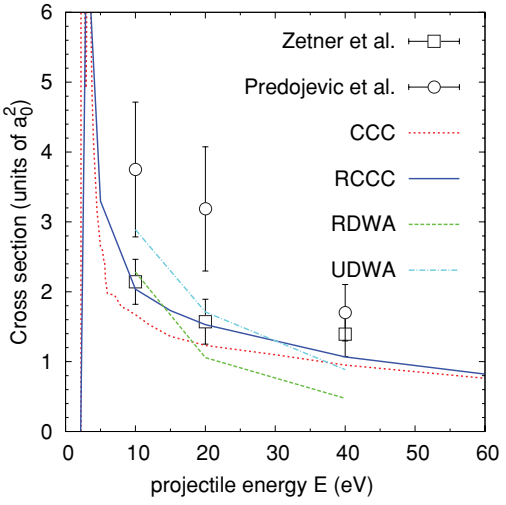

FIG. 7. (Color online) ICS for excitation of the $(6s6p)^3P_1^o$ state from the ground state of ytterbium. The measurements are from Predojević *et al.* [7] and Johnson *et al.* [8]. The RCCC and CCC calculations are described in the text, the UDWA calculations are presented in Johnson *et al.* [8], and the RDWA calculations are from Srivastava *et al.* [9].

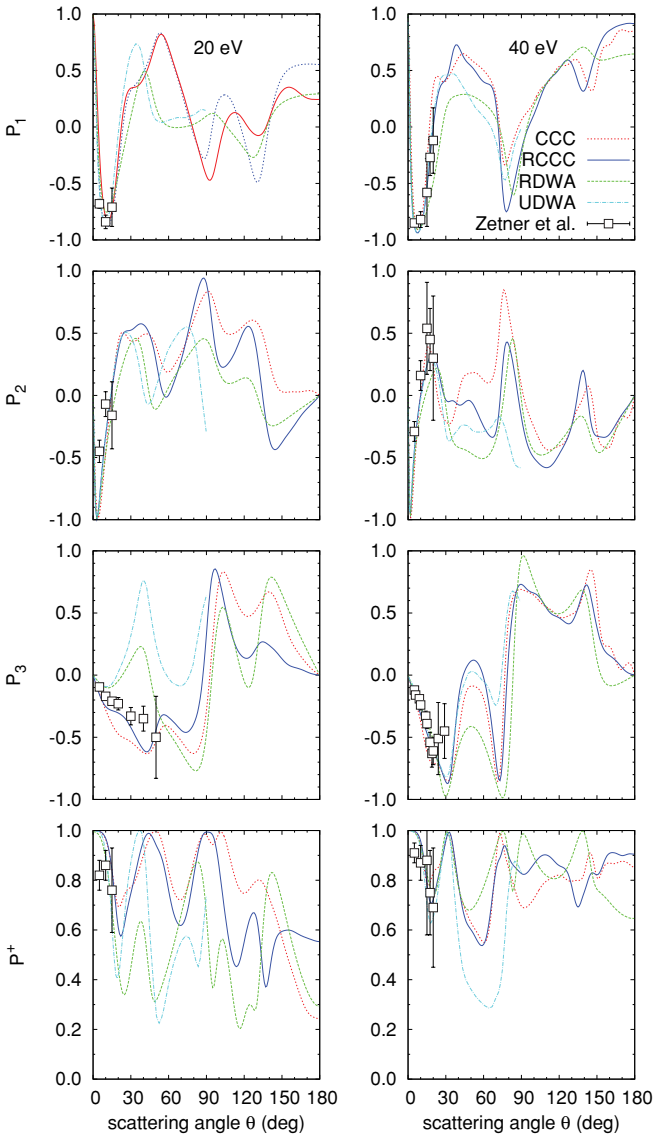

FIG. 8. (Color online) Stokes parameters P_1, P_2, and P_3, and degree of polarization P^+, for excitation of the $(6s6p)^3P_1^o$ state from the ground state of ytterbium at 20 and 40 eV incident electron energies. The measurements are from Zetner *et al.* [4]. The RCCC and CCC calculations are described in the text, and the RDWA calculations are from Srivastava *et al.* [9].

with the experimental measurements of Predojević *et al.* [6] at forward-scattering angles, however, at intermediate and large scattering angles, the situation is somewhat mixed. The RCCC and CCC results are also in good agreement with the complex optical potential (COP) calculations of Kelemen *et al.* [11], in particular at forward-scattering angles. At larger scattering angles, our results agree with the COP results in the number and position of DCS minima and maxima, but often disagree in absolute values. We noted earlier that our structure model substantially underestimates the Yb atom static dipole polarizability. Good agreement for forward-scattering DCS with experimental results, and in particular with COP results, is somewhat surprising as the COP method uses a polarization potential with $\alpha_D = 167.84$ for the static dipole polarizability of the Yb atom.

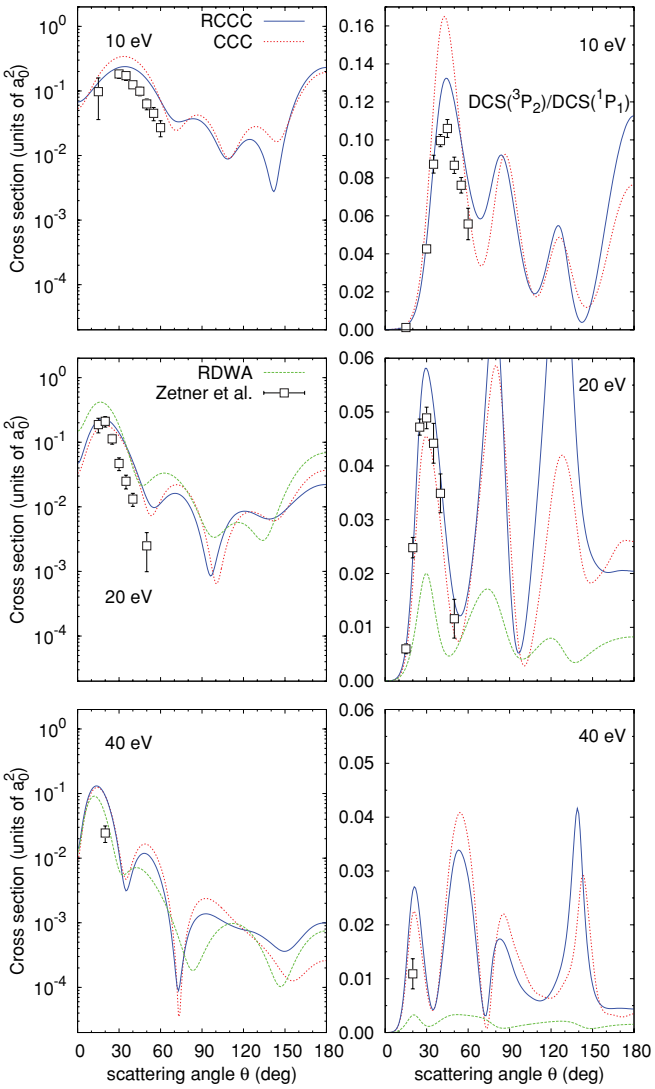

FIG. 9. (Color online) DCS for excitation of the $(6s6p)^3P_2^o$ state from the ground state of ytterbium and its ratio to the $(6s6p)^1P_1^o$ state DCS at 10, 20, and 40 eV incident electron energies. The measurements are from Zetner *et al.* [4]. The RCCC and CCC calculations are described in the text, the UDWA calculations are presented in Zetner *et al.* [4], and the RDWA calculations are from Srivastava *et al.* [9].

Figure 5 presents the integrated cross section for elastic scattering on the ground state of ytterbium. There is generally good agreement between the RCCC, CCC, and Predojević *et al.* [7] measurements, and the complex optical potential calculations are from [11]. There is poorer agreement with the calculations of Neerja *et al.* [12], who also employed a complex optical potential approximation.

In Fig. 6 we present differential cross sections for excitation of the $(6s6p)^3P_1^o$ state from the ground state of ytterbium and also the ratio $(6s6p)^3P_1^o$:$(6s6p)^1P_1^o$ DCS at 10, 20, and 40 eV incident electron energies. There is overall good agreement between the RCCC and CCC DCS results, except at 10 eV for small scattering angles where the CCC results are lower by approximately a factor of five. This is most likely an indication of inaccuracy in the semirelativistic corrections to the nonrelativistic CCC approach for this transition. For the

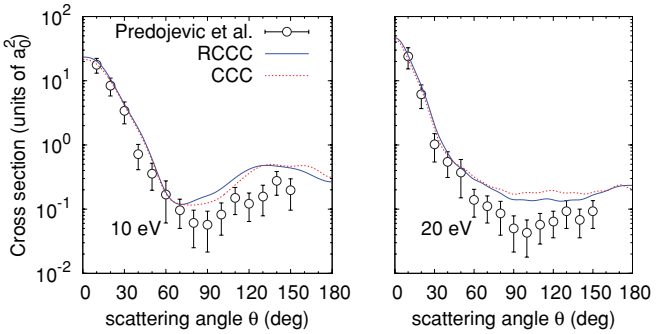

FIG. 10. (Color online) DCS for excitation of the $(6s5d)^1D_2^e$ state from the ground state of ytterbium at 10 and 20 eV incident electron energies. The measurements are from Predojević *et al.* [7]. The RCCC and CCC calculations are described in the text.

DCS at 10 and 20 eV for angles up to 30°, there is good agreement between the RCCC results and the experimental measurements of Predojević *et al.* [7] and Zetner *et al.* [4]. At larger angles, the agreement is poorer. For the DCS at 40 eV, there is good agreement between the RCCC results and the experimental measurements across a wider range of angles. The experimental $(6s6p)^3P_1^o$:$(6s6p)^1P_1^o$ DCS ratio measurements are not affected by the choice of normalization to absolute values, and at small scattering angles are in good agreement with the RCCC results. The CCC results, however, are not in agreement with the RCCC or experimental results at low angles for the ratio, which is once again an indication of inaccuracy in the semirelativistic approach. For larger angles at 10 and 20 eV, the experimental measurements of the ratio are in relatively good agreement with the RCCC results, however, there are discrepancies at 40 eV for the ratio at larger angles. There are significant discrepancies for the $(6s6p)^3P_1^o$:$(6s6p)^1P_1^o$ DCS ratio at all energies between the RCCC results and the UDWA [4] and RDWA [9] results. However, note that an updated RDWA calculation at 20 eV is presented in [1] that is in somewhat better agreement with the RCCC results.

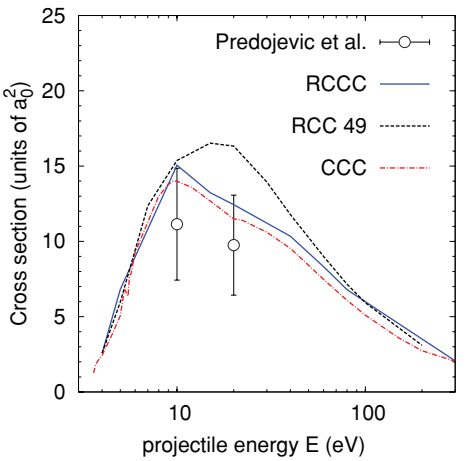

FIG. 11. (Color online) ICS for excitation of the $(6s5d)^1D_2^e$ state from the ground state of ytterbium. The RCCC and CCC calculations are described in the text, and measurements are from Predojević *et al.* [7].

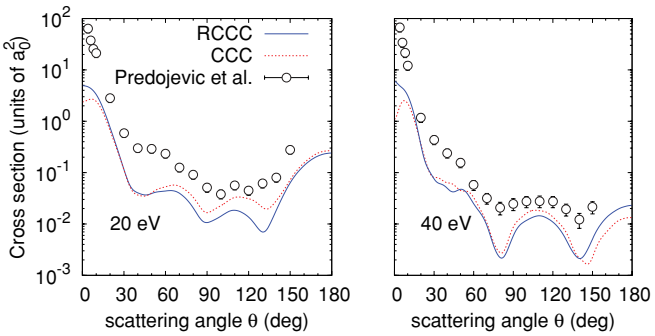

FIG. 12. (Color online) DCS for excitation of the $(6s7p)^1P_1^o$ state from the ground state of ytterbium at 20 and 40 eV incident electron energies. The measurements are from Predojević *et al.* [7]. The RCCC and CCC calculations are described in the text.

In Fig. 7 the ICS for the excitation of the $(6s6p)^3P_1^o$ state are presented. The RCCC results are larger than the CCC results, once again indicating a possible inaccuracy in the semirelativistic corrections to the nonrelativistic CCC method for this transition. The RCCC results are in good agreement with the experimental measurements from Johnson *et al.* [8], but not with the measurements from Predojević *et al.* [7]. This could be due to the difficulty in obtaining ICS values from experimental DCS measurements. In particular, numerical integration over small and large scattering angles requires polynomial extrapolation of the DCS.

Stokes parameters P_1, P_2, and P_3, and degree of polarization P^+, for excitation of the $(6s6p)^3P_1^o$ state from the ground state of ytterbium at 20 and 40 eV incident electron energies are presented in Fig. 8. The RCCC and CCC results are generally in good agreement with each other and with the measurements from Zetner *et al.* [4]. There is also good agreement with the UDWA calculations presented in Zetner *et al.* [4], and the RDWA calculations from Srivastava *et al.* [9].

The DCS for excitation of the $(6s6p)^3P_2^o$ state from the ground state of ytterbium and its ratio to the $(6s6p)^1P_1^o$ state DCS at 10, 20, and 40 eV incident electron energies

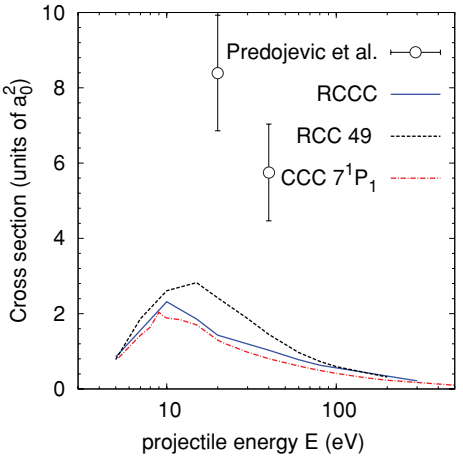

FIG. 13. (Color online) ICS for excitation of the $(6s7p)^1P_1^o$ state from the ground state of ytterbium. The measurements are from Predojević *et al.* [7]. The RCCC and CCC calculations are described in the text.

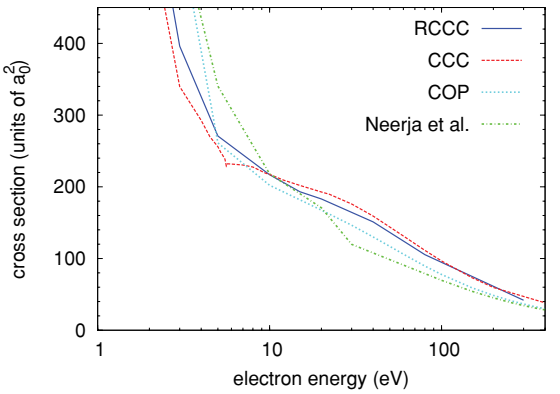

FIG. 14. (Color online) CCC and RCCC total cross sections. Also shown are the complex optical potential (COP) calculations from Kelemen *et al.* [11], and calculations from Neerja *et al.* [12].

are presented in Fig. 9. We note good agreement with the measurements of Zetner *et al.* [4] and the UDWA calculations, while the RDWA cross sections show somewhat different behavior.

In Fig. 10 the DCS for excitation of the $(6s5d)^1D_2^e$ state from the ground state of ytterbium at 10 and 20 eV incident electron energies are presented and compared with the measurements from Predojević *et al.* [7]. We find good agreement between the RCCC and CCC results, however, at larger scattering angles, both theories have cross sections that are larger than the experimental results. The integrated cross section for excitation of the $(6s5d)^1D_2^e$ state is presented in Fig. 11. The RCCC and CCC results are in good agreement with each other and with the measurements from Predojević *et al.* [7]. The effect of coupling to the continuum is shown, with a larger ICS for the RCC 49 calculation, which only includes bound states.

Differential cross sections for excitation of the $(6s7p)^1P_1^o$ state from the ground state at 20 and 40 eV incident electron energies are presented in Fig. 12 and compared with the measurements of Predojević *et al.* [7]. At both 20 and 40 eV, the CCC results are lower than the RCCC results for small

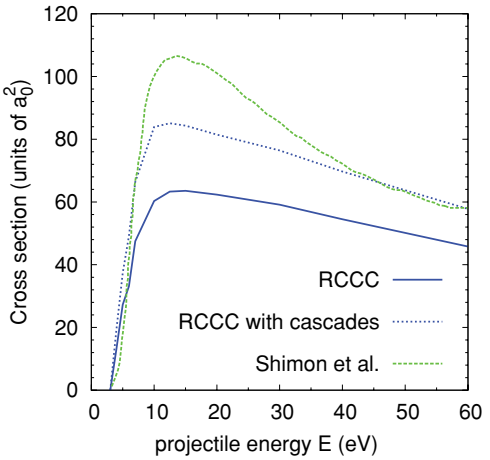

FIG. 15. (Color online) RCCC direct and cascade-corrected excitation cross sections for the $(6s6p)^1P_1^o$ state compared to the optical excitation function of Shimon *et al.* [5].

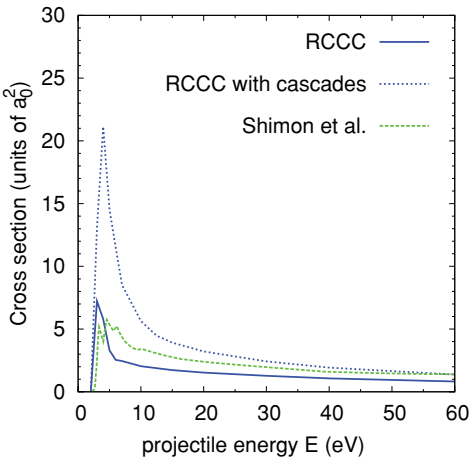

FIG. 16. (Color online) RCCC direct and cascade-corrected excitation cross sections for the $(6s6p)^3P_1^o$ state compared to the optical excitation function of Shimon *et al.* [5].

scattering angles. Otherwise there is relatively good agreement between the RCCC an CCC results, except for the 20 eV results in the range 60°–140° where the CCC results are larger than the RCCC results. Both the RCCC and CCC calculations are significantly lower than the experimental measurements of Predojević *et al.* [7] across all scattering angles. This could be a consequence of the current target structure model, which does not permit opening of the [Xe]$4f^{14}$ frozen core. The RCCC OOS value for the $(6s7p)^1P_1^o$–$(6s^2)^1S_0$ transition is 0.005, which is much lower than the experimental [24] value of 0.25.

Similarly, in Fig. 13, for the integrated cross section for excitation of the $(6s7p)^1P_1^o$ state, there is excellent agreement between the RCCC and CCC results, however, there is significant disagreement with the experimental measurements, which are much larger than the calculated cross sections. Once again this could be a consequence of the current model, which does not permit opening of the [Xe]$4f^{14}$ frozen core. The effect of coupling to the continuum is shown, with a larger ICS for the RCC 49 calculation, which only includes bound states and therefore does not include coupling to the continuum.

The total cross section is shown in Fig. 14. There is good agreement between the RCCC and CCC results, and also generally good agreement with the complex optical potential calculations of Kelemen *et al.* [11] and Neerja *et al.* [12].

The optical excitation function of the $(6s6p)^1P_1^o$ state measured by Shimon *et al.* [5] is shown in Fig. 15 and compared with the RCCC results, both direct and cascade corrected. A description of the calculation of cascade-corrected cross sections is given in [17]. The optical excitation function data has been normalized to the cascade-corrected RCCC results at high energy. The effect of cascades is to increase the cross section significantly. We note a difference in the shape of the optical excitation function in comparison with both RCCC results. The corresponding results for the $(6s6p)^3P_1^o$ state are shown in Fig. 16, where once again the optical excitation function data has been normalized to the cascade-corrected RCCC results at high energy. The RCCC cross sections increase at low energies in a manner similar to the measured optical excitation function, however, there are significant differences in the magnitudes of the RCCC direct and cascade-corrected results in comparison to the optical excitation function.

IV. CONCLUSION

We have used relativistic and nonrelativistic formulations of the convergent close-coupling method to calculate differential and integrated cross sections for electron scattering on Yb for elastic scattering and excitation of the states $(6s6p)^3P_{0,1,2}$, $(6s6p)^1P_1^o$, $(6s7p)^1P_1^o$, and $(6s5d)^1D_2^e$ for a range of incident electron energies. We have also presented calculations of the total cross section, and angle-differential Stokes parameters for excitation of the $(6s6p)^3P_1^o$ state from the ground state. The results have been compared with experimental data where available. In general we found very good agreement between the RCCC and CCC (with semirelativistic corrections) results indicating that relativistic effects do not dominate except for the $(6s6p)^3P_1^o$ DCS at forward-scattering angles, which indicates that the fully relativistic RCCC formalism is more accurate in this case. Discrepancies exist between experiments and we found that the previous normalization of the $(6s6p)^1P_1^o$ DCS by Johnson *et al.* [8] using the UDWA ICS value for the $(6s6p)^1P_1^o$ state at 80 eV has resulted in disagreement with the RCCC and CCC results, particularly at low and intermediate energies. We have presented renormalization scale factors for a better comparison of our results with the experimental data. We found that renormalized experimental results are generally in better agreement with present close-coupling calculations than with previous first-order calculations. However, the agreement at incident electron energies below 40 eV is not satisfactory. This is somewhat similar to the case of electron scattering from the excited states of ytterbium [1,2]. Further detailed and accurate theoretical and experimental investigations are required to improve our understanding of electron scattering from ytterbium.

ACKNOWLEDGMENTS

Support of the Australian Research Council and Curtin University is acknowledged. We are grateful for access to the Australian National Computational Infrastructure and its Western Australian node, iVEC.

[1] J. D. Hein, S. Kidwai, P. W. Zetner, C. Bostock, D. V. Fursa, I. Bray, L. Sharma, R. Srivastava, and A. Stauffer, J. Phys. B **44**, 015202 (2011).

[2] J. D. Hein, S. Kidwai, P. W. Zetner, C. Bostock, D. V. Fursa, I. Bray, L. Sharma, R. Srivastava, and A. Stauffer, J. Phys. B **44**, 075201 (2011).

[3] Y. Li and P. W. Zetner, J. Phys. B **27**, L293 (1994).
[4] P. W. Zetner, P. V. Johnson, G. Csanak, R. E. H. Clark, and J. Abdallah Jr., J. Phys. B **34**, 1619 (2001).
[5] L. L. Shimon, N. V. Golovchak, I. I. Garga, and I. V. Kurta, Opt. Spektrosk. **50**, 1037 (1981).
[6] B. Predojević, D. Šević, V. Pejčev, B. P. Marinković, and D. M. Filipović, J. Phys. B **38**, 1329 (2005).
[7] B. Predojević, D. Šević, V. Pejčev, B. P. Marinković, and D. M. Filipović, J. Phys. B **38**, 3489 (2005).
[8] P. V. Johnson, Y. Li, P. W. Zetner, G. Csanak, R. E. H. Clark, and J. Abdallah Jr., J. Phys. B **31**, 3027 (1998).
[9] R. Srivastava, R. P. McEachran, and A. D. Stauffer, J. Phys. B **28**, 885 (1995).
[10] V. I. Kelemen, M. M. Dovhanych, and E. Y. Remeta, J. Phys. B **41**, 035204 (2008).
[11] V. I. Kelemen, M. M. Dovhanych, and E. Y. Remeta, J. Phys. B **41**, 125202 (2008).
[12] Neerja, A. N. Tripathi, and A. K. Jain, Phys. Rev. A **61**, 032713 (2000).
[13] D. V. Fursa and I. Bray, Phys. Rev. Lett. **100**, 113201 (2008).
[14] D. V. Fursa, C. J. Bostock, and I. Bray, Phys. Rev. A **80**, 022717 (2009).
[15] D. V. Fursa and I. Bray, J. Phys. Conf. Ser. **185**, 012008 (2009).
[16] M. Maslov, M. J. Brunger, P. J. O. Teubner, O. Zatsarinny, K. Bartschat, D. Fursa, I. Bray, and R. P. McEachran, Phys. Rev. A **77**, 062711 (2008).
[17] C. J. Bostock, D. V. Fursa, and I. Bray, Phys. Rev. A **80**, 052708 (2009).
[18] C. J. Bostock, D. V. Fursa, and I. Bray, Phys. Rev. A **82**, 022713 (2010).
[19] K. G. Dyall, I. P. Grant, C. T. Johnson, F. P. Parpia, and E. P. Plummer, Comput. Phys. Commun. **55**, 425 (1989).
[20] I. P. Grant and H. M. Quiney, Phys. Rev. A **62**, 022508 (2000).
[21] D. V. Fursa, I. Bray, and G. Lister, J. Phys. B **36**, 4255 (2003).
[22] D. V. Fursa and I. Bray, J. Phys. B **30**, 5895 (1997).
[23] L. V. Chernysheva, N. A. Cherepkov, and V. Radojevic, Comput. Phys. Commun. **11**, 57 (1976).
[24] [http://physics.nist.gov/PhysRefData/ASD/levels_form.html].
[25] B. Budick and J. Snir, Phys. Rev. A **1**, 545 (1970).
[26] N. Penkin and V. A. Komaroski, J. Quantum Spectrosc. Radiat. Transfer **16**, 217 (1976).
[27] W. Lange, Phys. Lett. **20**, 166 (1966).
[28] M. Baumann and G. Wandel, Phys. Lett. **22**, 283 (1966).
[29] P. Zhang and A. Dalgarno, J. Phys. Chem. A **111**, 12471 (2007).
[30] V. A. Dzuba and A. Derevianko, J. Phys. B **43**, 074011 (2010).
[31] K. Bartschat, D. V. Fursa, and I. Bray, J. Phys. B **43**, 125202 (2010).
[32] Z. Felfli and A. Z. Msezane, J. Phys. B **31**, L165 (1998).
[33] N. B. Avdonina, Z. Felfli, D. V. Fursa, and A. Z. Msezane, Phys. Rev. A **62**, 014703 (2000).